Macromolecules

pubs.acs.org/Macromolecules Article

Closed-Loop Phase Behavior of Nonstoichiometric Coacervates in Coarse-Grained Simulations

Sai Vineeth Bobbili and Scott T. Milner*

Cite This: *Macromolecules* 2022, 55, 511−516 Read Online

ACCESS | Metrics & More | Article Recommendations

ABSTRACT: Most studies of polyelectrolyte coacervate phase behavior focus on symmetric mixtures of oppositely charged polymers. Here we use a coarse-grained simulation, in which all bonded monomers and mobile counterions are represented as Lennard-Jones particles with unit charge and diameter equal to the Bjerrum length, to study the impact of charge asymmetry on coacervate phase behavior. We study the impact of salt on the concentration of polymers and mobile ions in each phase and qualitatively reproduce the closed-loop behavior observed in recent experiments on nonstoichiometric coacervates. We find that the counterions from added salt distribute unevenly, preferring the dilute phase to maximize their translational entropy, analogous to Donnan equilibrium for a charged membrane. The coacervate phase shrinks under osmotic pressure, leading to increased polymer concentration with small amounts of added salt.

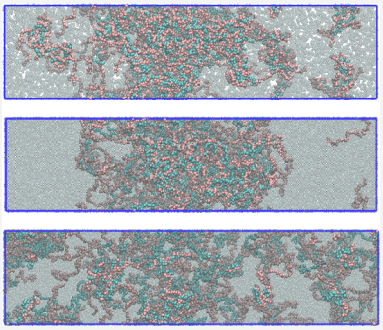

INTRODUCTION

Mixing oppositely charged polyelectrolytes results in associative phase separation into a polymer-rich coacervate and a dilute supernatant phase. Such materials are of interest for applications in protein encapsulation,[1−4] adhesives,[5−9] and food products.[10−12] Coacervates are also of interest in cellular biology as an element in the formation of membraneless organelles.[13−18]

Most studies of coacervate phase behavior, whether experiments[19−21] or simulations,[22−24] using rheology,[25−28] polymer conformations,[29,30] or interfacial tension[31,32] focus on charge-stoichiometric mixtures, with equal and opposite total charge on the polycations and polyanions.

This charge symmetry can be broken in multiple ways: by varying the fraction of charged monomers on a chain,[33] or the chain lengths,[34] or mixing nonstoichiometric proportions of oppositely charged polymers.[18,33] In any charge-asymmetric coacervate, there will be sufficient counterions to maintain overall charge neutrality. For sufficient asymmetry, coacervates are not observed to form.[35]

Asymmetric coacervates have applications in separating biomolecules. van Lente et al.[18] used asymmetric polyelectrolyte complexes to separate two structurally similar but oppositely charged proteins. Priftis et al.[36] investigated the effects of stoichiometry and pH on salt resistance and the viscoelastic behavior of ternary polyelectrolyte coacervates using turbidity and rheological measurements.

A challenge in studying asymmetric coacervates is measuring phase concentrations of each species. Recently, Friedowitz et al.[37] used fluorescent labeled polyelectrolytes with inductively coupled plasma mass spectroscopy to investigate nonstoichiometric coacervates. Their phase diagram exhibits "looping in" behavior, in which the polymer concentration in the coacervate first increases with addition of salt and then decreases as more salt is added, eventually forming a one-phase solution. They explain that counterions from low added salt prefer the dilute phase to maximize their mixing entropy, avoiding the high concentration of mobile counterions trapped in the asymmetric coacervate, analogous to rejection of salt solutions by charged membranes under Donnan equilibrium.[38] The coacervate then balances the osmotic pressure between the two phases by expelling water, which increases the polymer concentration in the coacervate.

The phase diagram for nonstoichiometric coacervates by Friedowitz et al. also shows other characteristic features: (a) the two-phase region narrows with increase in asymmetry, (b) the critical salt concentration decreases slightly with asymmetry, and (c) for low salt concentrations, the concentration of free ions in the coacervate is higher than in the dilute phase. A small increase in polymer concentration for asymmetric coacervates with low added salt was also reported by Li et al.[39] in their study of the effect of pH on polyelectrolyte charging and resulting coacervate phase behavior.

Several recent theoretical and computational studies have focused on asymmetric coacervates. Zhang et al.[40] use liquid

Received: October 13, 2021
Revised: December 20, 2021
Published: January 10, 2022

https://doi.org/10.1021/acs.macromol.1c02115
Macromolecules 2022, 55, 511−516

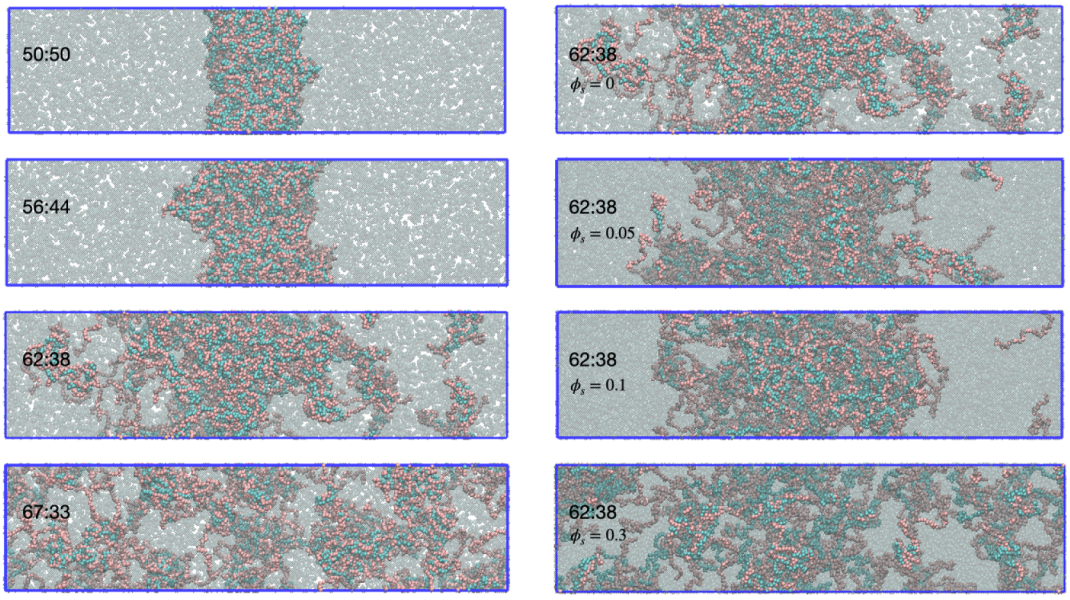

Figure 1. Simulation snapshots show (left) the impact of mixing ratio of polycations:polyanions without added salt and (right) the impact of adding salt. Without added salt, mixing 62 polycations and 38 polyanions results in two-phase coexistence (top right). As salt is added, the polymer-rich phase first becomes more concentrated (second and third on right) and then swells to form a single phase (bottom right). Polycations and polyanions are shown as pink and blue beads; free ions are translucent.

state theory to construct a three-dimensional phase diagram in terms of individual component concentrations. For small asymmetry in polymer concentrations, they show that the two-phase becomes narrower, which they attribute to the translational entropy of the excess counterions needed for charge neutrality. Adhikari et al.[34] use mean field theory to compute phase diagrams that capture effects of charge asymmetry from different chain lengths as well as non-stoichiometric mixtures. In addition to excess counterions being present to maintain electroneutrality, they attribute the closed-loop behavior to a decrease in dipole−dipole attractions and increase in charge repulsions with asymmetry. Rubinstein et al.[41,42] provide a scaling theory for the effect of salt and electrostatic strength on structure of coacervates with asymmetric charge densities. They predict that charge-asymmetric weak coacervates form double solutions with two correlation lengths, while strongly asymmetric coacervates can form bottlebrush or star-like gels. Knoerdel et al.[33] use a transfer matrix model to obtain phase diagrams that predict the impact of charge asymmetry through changing solution pH and stoichiometry; however, unlike experiments, they do not find closed-loop behavior in their phase diagrams.

In our previous work,[43] we introduced a simple simulation model to obtain coacervate phase diagrams. In our bead−spring model, all ions on polymers, dissociated counterions, and ions from the added salt are represented by beads of unit charge and diameter equal to the Bjerrum length. This choice of diameter avoids counterion condensation in our simulations.[44] We measured density profiles of a slab of coacervate phase in equilibrium with dilute phase to obtain polymer and mobile ion concentrations in each phase and construct a phase diagram, describing the salt and polymer concentrations in each phase. For symmetric coacervates, with addition of salt, the polymer concentration in the coacervate phase decreases. We found that the total ion concentration in the coacervate remained constant with addition of salt. That is, with the addition of salt, the newly added ions distribute nearly uniformly through both the coacervate and dilute phases, since the electrostatic interaction of each ion in the coacervate is only of the order of kT. Hence, added salt swells the coacervate in coexistence with excess solvent, but only by the average volume fraction of mobile ions throughout the system. This is also a robust feature in published experimental phase diagrams. Additionally, this model can also be adjusted for different monomer sizes and interactions between polymers (as a proxy for solvent quality).

In this work, we use our model to study nonstoichiometric coacervates. We first vary the "mixing ratio", i.e., the ratio of polycation and polyanion chains of equal length and charge densities, to investigate the impact of asymmetry on phase behavior. We then add salt to such nonstoichiometric systems and find a closed-loop phase behavior, which we compare to recent experimental results on synthetic polyacrylamide coacervates.[37] Although there are different ways of breaking symmetry as mentioned above, in this work, we introduce asymmetry only by varying stoichiometry.

METHODS

In our bead−spring model,[43] all polymer beads and mobile counterions interact with repulsive Lennard-Jones interactions (eq 1).

$$U_{\mathrm{LJ}}(r) = \begin{cases} 4\epsilon\left(\left(\frac{\sigma}{r}\right)^{12} - \left(\frac{\sigma}{r}\right)^{6}\right) + \epsilon & r \le r_{\mathrm{c}} \\ 0 & r \ge r_{\mathrm{c}} \end{cases} \quad (1)$$

Here $\epsilon = kT$ (2.49 kJ/mol at 300 K). The potential between bonded beads is a stiff harmonic spring, given by

$$U_{\mathrm{bond}}(r) = (1/2)k_{\mathrm{b}}(r - r_0)^2 \quad (2)$$

where $r_0 = 2^{1/6}\sigma$ and the spring constant k_{b} equals 400 kT/σ^2.

Each bead carries a unit charge, with the Coulomb interaction between beads given by

https://doi.org/10.1021/acs.macromol.1c02115
Macromolecules 2022, 55, 511−516

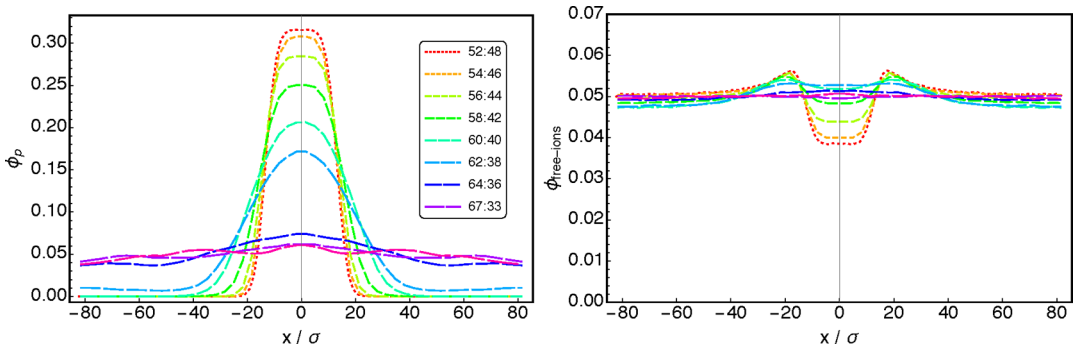

Figure 2. Density profiles of polymers (left) and free ions (right) show the impact of asymmetry on concentration in the coacervate and dilute phases.

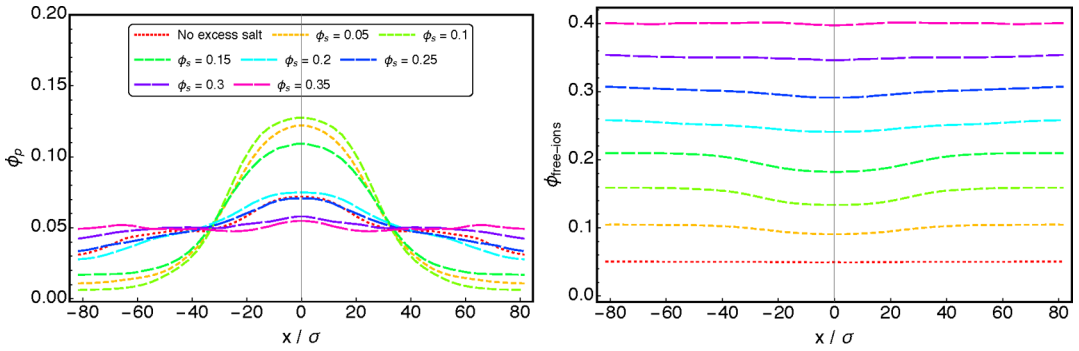

Figure 3. Density profiles of polymers (left) and free ions (right) show the impact of added salt on their concentrations in the coacervate and dilute phases. Without added salt ($\phi_s = 0$), there are oppositely charged counterions for each monomer on all the polymers.

$$U_{Coul}(r) = kTl_B\frac{z_1z_2}{r} \quad (3)$$

Here l_B is the Bjerrum length, z_1 and z_2 are the valencies (±1), and r is the separation distance. We set the effective bead diameter $2^{1/6}\sigma$ equal to the Bjerrum length. We use particle-mesh Ewald methods to compute Coulomb interactions.

We set the total polymer concentration in the simulation box such that the number density of monomer beads is a fraction ϕ_p times $\phi_m = 0.7/\sigma^3$, and $\phi_p = 0.05$. The concentration ϕ_m we have previously adopted as a "melt" concentration in charge-neutral bead–spring systems.[45] Here, we report ϕ as the volume fraction relative to ϕ_m.

We introduce asymmetry by adding different amounts of structurally identical but oppositely charged polyelectrolytes. Our polymer chains have length $N = 100$ beads. We vary the number of chains from 50 polycations and 50 polyanions up to 67 polycations and 33 polyanions. With no added salt ($\phi_s = 0$), our system includes oppositely charged counterions for each monomer on all the polymers. We add salt as additional oppositely charged free ion pairs.

We start our simulations from a phase-separated configuration, built as a slab in the center of the simulation box, populated by initial random walk configurations for the chains. To aid in measuring density profiles, we gently restrain the polymer center of mass to the center of the simulation box with an umbrella potential of spring constant 16 kT/σ^2, in the direction normal to the phase boundary.

For computational efficiency we use implicit solvent; correspondingly, we use stochastic dynamics, in which random forces added to particle velocities cause them to diffuse as collisions with real solvent would do. All beads interact with purely repulsive Lennard-Jones potentials, which correspond to good solvent conditions. After initial energy minimization, we run NVT simulations for 3×10^8 time steps. Our time step is 0.00228τ, where τ is the Lennard-Jones time $\sigma(m/\epsilon)^{1/2}$. The phases equilibrate in less than 5×10^7 time steps (symmetric systems take much less time). We measure symmetrized density profiles of polymers and counterions over the final 2×10^8 time steps, from which we infer the phase diagram. We use Gromacs for our simulations and density profile analysis.[46]

RESULTS AND DISCUSSION

The coacervate phase becomes less cohesive as the asymmetry increases, as shown in Figure 1 (left). Mixtures of oppositely charged polyelectrolytes with charge stoichiometry undergo associative phase separation into a polymer-rich coacervate phase and a dilute supernatant phase (top snapshot in Figure 1 (left)). As the mixtures become asymmetric, the coacervate phase swells, and the polymer chains begin to enter the dilute phase. With sufficient charge asymmetry, the coacervate dissolves into a single phase (bottom snapshot in Figure 1 (left)).

With addition of salt to the nonstoichiometric mixture, the coacervate phase first shrinks in the low-salt regime and then swells with further addition of salt (see Figure 1 (right)). This behavior is consistent with experiments of Friedowitz et al.[37] using coacervates of synthetic polyacrylamides. Shrinking with low added salt is not observed for symmetrically charged coacervates, which only swell as salt is added.

Density profiles (Figures 2 and 3) quantify our observations from the simulation snapshots. Density profiles show that the polymer concentration in the center of the simulation box decreases with increasing asymmetry, until a single phase results (Figure 2 (left)). Symmetric coacervates exhibit a sharp

https://doi.org/10.1021/acs.macromol.1c02115
Macromolecules 2022, 55, 511−516

interface between the concentrated and dilute phases, while asymmetric systems display a much broader interface, implying that the coacervate phase is less cohesive and the dilute phase not completely devoid of polymers.

For symmetric mixtures of polycations and polyanions, there is a favorable partition of counterions to the dilute phase, as reported by previous experiments[19] and simulations.[23,24] With charge asymmetry, additional mobile counterions must reside in the coacervate to maintain charge neutrality. Figure 2 (right) shows that the free ion concentration is higher in the dilute phase when the system is nearly symmetric, with the mixing ratio up to 56:44. As the asymmetry increases (up to the mixing ratio 62:38), the free ion concentration in the coacervate phase becomes slightly higher than in the dilute phase. For example, the free ion concentration for the 62:38 ratio is slightly higher than 0.05 in the concentrated phase and less than 0.05 in the dilute phase. For sufficiently asymmetric systems (64:36 and above), a single phase results, as the counterion osmotic pressure in the coacervate becomes large enough to destabilize the phase.

Symmetrically charged coacervates swell with addition of salt. But for asymmetric coacervates, density profiles in Figure 3 (left) show that the polymer concentration first increases with added salt and then decreases until a single phase results. Here, the highest polymer concentration in the coacervate phase is observed at $\phi_s = 0.1$. Density profiles of counterions in Figure 3 (right) show that added salt at low concentrations slightly prefers to enter the dilute phase, as evident from the troughs in the low salt regime between $\phi_s = 0.05$ and 0.15. Although this effect is modest in magnitude, we acknowledge the cause and the impact it has on osmotic pressure, discussed further below.

The coacervate phase diagram (Figure 4) displays a striking evolution as charge asymmetry increases. For sufficiently

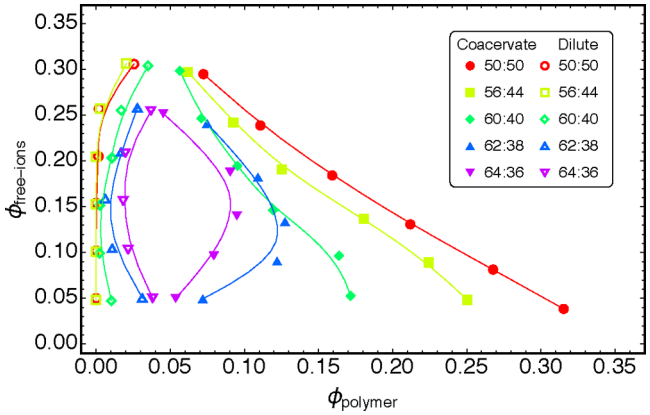

Figure 4. Phase diagram shows the impact of added salt on concentration of polymers and free ions in each phase.

asymmetric systems the two-phase region becomes narrower, and a closed-loop behavior results, indicating that the polymer concentration in the coacervate first increases with added salt and then decreases as more salt is added. The amount of salt needed to obtain a single phase is progressively less for more asymmetric coacervates. All these features are consistent with experimental observations.

Nonstoichiometry leads to "polymer overcharging"; that is, the coacervate phase contains more of whichever polyelectrolyte we added in greater quantity. Figure 5 displays the concentrations of each polyion species separately (blue for polyanion, red for polycation) in the dilute and concentrated phases versus the total mobile ion concentration in the phase. Because the coacervate phase is overall charge neutral, we can infer from Figure 5 that excess mobile anions are required to maintain neutrality in each phase, which is larger for more asymmetric systems. We notice that at high asymmetry there are more polycations in the dilute phase, where they presumably flee to relax somewhat the asymmetry in the concentrated phase and release captive mobile anions from the coacervate.

In stoichiometric coacervates, both phases are equally hospitable for added salt ions. Hence, the coacervate phase swells with added salt, but only by the average salt concentration; the symmetric coacervate remains essentially a "Bjerrum liquid" of polyelectrolyte chains plus mobile ions at a constant melt concentration. In contrast, the total ion concentration in nonstoichiometric coacervates does not remain constant (Figure 6) below the critical salt concentration. Instead, small amounts of added salt increase the total ion concentration in the coacervate, as shown in Figure 6.

The physical explanation presented by Friedowitz et al.[37] is consistent with our observations. Asymmetric coacervates with more polycations than polyanions retain extra mobile anions to maintain charge neutrality (see Figure 2). In the low salt regime, the high anion concentration in the coacervate tends to repel salt with the same anion because the translational entropy of added anions is larger in the dilute phase than in the coacervate. This mechanism is the same as for charged membranes, which repel added salt with the same counterion until the concentration approaches the membrane charge density, described by Donnan equilibrium.[38]

Because the first added salt goes more to the dilute phase, the osmotic pressure there increases. To balance the osmotic pressure, the coacervate expels water, becoming more concentrated. As the salt concentration increases to be comparable to the anion concentration in the coacervate, salt is no longer rejected from the coacervate, which begins to swell from the added salt just as a symmetric coacervate would.

Some of these observations were noted in some previous studies as well. Zhang et al.[40] study the effect of concentration asymmetry using liquid state theory. They report a shrinkage of the phase diagram in asymmetric mixtures of polyelectrolytes. This work does not, however, report a closed-loop behavior. We speculate this may be due to small range of asymmetry considered while constructing the phase diagram. Danielsen et al.[47] observe a similar closed loop behavior in their simulations for self-coacervation in polyampholyte mixtures at small asymmetries (up to 53:47). At high asymmetries (over 55:45), they observe development of tadpole configurations, as predicted by Rubinstein et al.[48,49] for charge asymmetric block polyampholytes.

CONCLUSION

We use molecular dynamics simulations to understand the impact of the "mixing ratio" (ratio of polycations and polyanions added) and added salt in nonstoichiometric coacervates. Charge asymmetry destabilizes the coacervate phase; sufficiently asymmetric mixtures result in a single phase. Stoichiometric coacervates exhibit "salting-in" behavior, in which the polymer concentration steadily decreases with added salt, which swells the coacervate at constant total ion concentration. In contrast, when polycations and polyanions

https://doi.org/10.1021/acs.macromol.1c02115
Macromolecules 2022, 55, 511−516

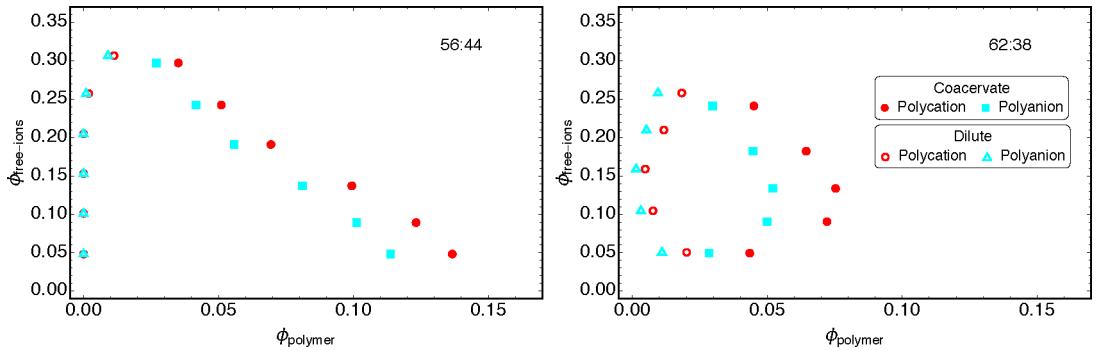

Figure 5. Phase diagram indicating polycation and polyanion concentrations separately for the mixing ratios of (left) 56:44 and (right) 62:38 (blue for polyanions, red for polycations).

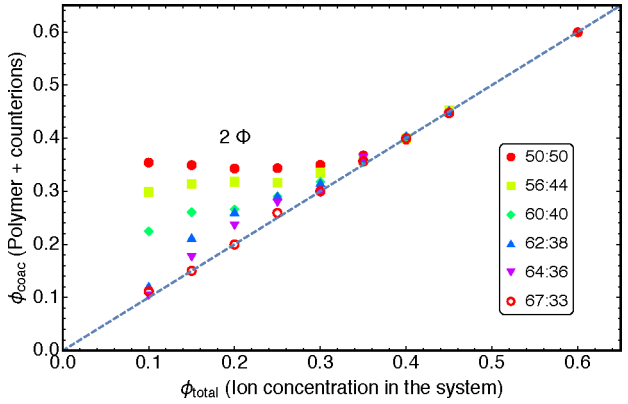

Figure 6. Ion concentration in coacervates with added salt; dashed line represents the one-phase region.

of equal length and charge per bead are mixed in non-stoichiometric proportions, the coacervate phase first shrinks as salt is added and then eventually swells with addition of more salt.

Our simulation phase diagram exhibits closed-loop behavior for sufficiently asymmetric coacervates. This behavior reflects the tendency of small amounts of added salt to prefer the dilute phase over the asymmetric coacervate. This preference results from the relatively high concentrations of mobile anions held there to neutralize the charge of the excess polycations, such that added salt has more translational entropy in the dilute phase than in the coacervate. This situation is very similar to Donnan equilibrium, in which a charged membrane holds mobile counterions in place and tends to reject salt with the same counterion until the salt concentration approaches the membrane charge density.

To balance the excess osmotic pressure from the rejected salt, the coacervate phase expels water, which shrinks the phase and increases the polymer concentration, leading to the characteristic "looping-in" behavior. Our simulation phase diagrams show all the characteristic features observed in recent experiments on synthetic polyacrylamides, including the narrowing of the two-phase region as charge asymmetry destabilizes the coacervate phase and a reduced critical point as less salt is needed to destabilize the asymmetric coacervate.

AUTHOR INFORMATION

Corresponding Author

Scott T. Milner − *Department of Chemical Engineering, The Pennsylvania State University, University Park, Pennsylvania 16802, United States;* orcid.org/0000-0002-9774-3307; Email: stm9@psu.edu

Author

Sai Vineeth Bobbili − *Department of Chemical Engineering, The Pennsylvania State University, University Park, Pennsylvania 16802, United States;* orcid.org/0000-0001-9694-605X

Complete contact information is available at: https://pubs.acs.org/10.1021/acs.macromol.1c02115

Notes

The authors declare no competing financial interest.

ACKNOWLEDGMENTS

The authors acknowledge financial support from the NSF under DMR-1905632.

REFERENCES

(1) Black, K. A.; Priftis, D.; Perry, S. L.; Yip, J.; Byun, W. Y.; Tirrell, M. Protein encapsulation via polypeptide complex coacervation. *ACS Macro Lett.* **2014**, *3*, 1088−1091.

(2) Obermeyer, A. C.; Mills, C. E.; Dong, X.-H.; Flores, R. J.; Olsen, B. D. Complex coacervation of supercharged proteins with polyelectrolytes. *Soft Matter* **2016**, *12*, 3570−3581.

(3) Nolles, A.; Westphal, A. H.; de Hoop, J. A.; Fokkink, R. G.; Kleijn, J. M.; van Berkel, W. J.; Borst, J. W. Encapsulation of GFP in complex coacervate core micelles. *Biomacromolecules* **2015**, *16*, 1542−1549.

(4) McTigue, W. C. B.; Perry, S. L. Design rules for encapsulating proteins into complex coacervates. *Soft Matter* **2019**, *15*, 3089−3103.

(5) Zhao, Q.; Lee, D. W.; Ahn, B. K.; Seo, S.; Kaufman, Y.; Israelachvili, J. N.; Waite, J. H. Underwater contact adhesion and microarchitecture in polyelectrolyte complexes actuated by solvent exchange. *Nat. Mater.* **2016**, *15*, 407−412.

(6) Stewart, R. J.; Wang, C. S.; Shao, H. Complex coacervates as a foundation for synthetic underwater adhesives. *Advances in colloid and interface science* **2011**, *167*, 85−93.

(7) Lim, S.; Moon, D.; Kim, H. J.; Seo, J. H.; Kang, I. S.; Cha, H. J. Interfacial tension of complex coacervated mussel adhesive protein according to the Hofmeister series. *Langmuir* **2014**, *30*, 1108−1115.

(8) Wang, W.; Xu, Y.; Li, A.; Li, T.; Liu, M.; von Klitzing, R.; Ober, C. K.; Kayitmazer, A. B.; Li, L.; Guo, X. Zinc induced polyelectrolyte coacervate bioadhesive and its transition to a self-healing hydrogel. *Rsc Advances* **2015**, *5*, 66871−66878.

(9) Winslow, B. D.; Shao, H.; Stewart, R. J.; Tresco, P. A. Biocompatibility of adhesive complex coacervates modeled after the sandcastle glue of Phragmatopoma californica for craniofacial reconstruction. *Biomaterials* **2010**, *31*, 9373−9381.

(10) Turgeon, S.; Schmitt, C.; Sanchez, C. Protein−polysaccharide complexes and coacervates. *Curr. Opin. Colloid Interface Sci.* **2007**, *12*, 166−178.
(11) Schmitt, C.; Turgeon, S. L. Protein/polysaccharide complexes and coacervates in food systems. *Advances in colloid and interface science* **2011**, *167*, 63−70.
(12) Matalanis, A.; Jones, O. G.; McClements, D. J. Structured biopolymer-based delivery systems for encapsulation, protection, and release of lipophilic compounds. *Food Hydrocolloids* **2011**, *25*, 1865−1880.
(13) Jia, T. Z.; Hentrich, C.; Szostak, J. W. Rapid RNA exchange in aqueous two-phase system and coacervate droplets. *Origins of Life and Evolution of Biospheres* **2014**, *44*, 1−12.
(14) Decker, C. J.; Parker, R. P-bodies and stress granules: possible roles in the control of translation and mRNA degradation. *Cold Spring Harbor perspectives in biology* **2012**, *4*, a012286.
(15) Sokolova, E.; Spruijt, E.; Hansen, M. M.; Dubuc, E.; Groen, J.; Chokkalingam, V.; Piruska, A.; Heus, H. A.; Huck, W. T. Enhanced transcription rates in membrane-free protocells formed by coacervation of cell lysate. *Proc. Natl. Acad. Sci. U. S. A.* **2013**, *110*, 11692−11697.
(16) Shin, Y.; Brangwynne, C. P. Liquid phase condensation in cell physiology and disease. *Science* **2017**, *357*, eaaf4382.
(17) Perry, S. L. Phase separation: Bridging polymer physics and biology. *Curr. Opin. Colloid Interface Sci.* **2019**, *39*, 86−97.
(18) Van Lente, J. J.; Claessens, M. M.; Lindhoud, S. Charge-based separation of proteins using polyelectrolyte complexes as models for membraneless organelles. *Biomacromolecules* **2019**, *20*, 3696−3703.
(19) Li, L.; Srivastava, S.; Andreev, M.; Marciel, A. B.; de Pablo, J. J.; Tirrell, M. V. Phase behavior and salt partitioning in polyelectrolyte complex coacervates. *Macromolecules* **2018**, *51*, 2988−2995.
(20) Spruijt, E.; Westphal, A. H.; Borst, J. W.; Cohen Stuart, M. A.; van der Gucht, J. Binodal compositions of polyelectrolyte complexes. *Macromolecules* **2010**, *43*, 6476−6484.
(21) Lou, J.; Friedowitz, S.; Qin, J.; Xia, Y. Tunable coacervation of well-defined homologous polyanions and polycations by local polarity. *ACS central science* **2019**, *5*, 549−557.
(22) Lytle, T. K.; Salazar, A. J.; Sing, C. E. Interfacial properties of polymeric complex coacervates from simulation and theory. *J. Chem. Phys.* **2018**, *149*, 163315.
(23) Radhakrishna, M.; Basu, K.; Liu, Y.; Shamsi, R.; Perry, S. L.; Sing, C. E. Molecular connectivity and correlation effects on polymer coacervation. *Macromolecules* **2017**, *50*, 3030−3037.
(24) Andreev, M.; Prabhu, V. M.; Douglas, J. F.; Tirrell, M.; de Pablo, J. J. Complex coacervation in polyelectrolytes from a coarse-grained model. *Macromolecules* **2018**, *51*, 6717−6723.
(25) Spruijt, E.; Sprakel, J.; Lemmers, M.; Cohen Stuart, M. A.; Van Der Gucht, J. Relaxation dynamics at different time scales in electrostatic complexes: time-salt superposition. *Phys. Rev. Lett.* **2010**, *105*, 208301.
(26) Spruijt, E.; Cohen Stuart, M. A.; van der Gucht, J. Linear viscoelasticity of polyelectrolyte complex coacervates. *Macromolecules* **2013**, *46*, 1633−1641.
(27) Huang, J.; Morin, F. J.; Laaser, J. E. Charge-density-dominated phase behavior and viscoelasticity of polyelectrolyte complex coacervates. *Macromolecules* **2019**, *52*, 4957−4967.
(28) Morin, F. J.; Puppo, M. L.; Laaser, J. Decoupling Salt-and Polymer-Dependent Dynamics in Polyelectrolyte Complex Coacervates via Salt Addition. *Soft Matter* **2021**, *17*, 1223−1231.
(29) Xie, S.; Zhang, B.; Mao, Y.; He, L.; Hong, K.; Bates, F. S.; Lodge, T. P. Influence of Added Salt on Chain Conformations in Poly (ethylene oxide) Melts: SANS Analysis with Complications. *Macromolecules* **2020**, *53*, 7141−7149.
(30) Marciel, A. B.; Srivastava, S.; Tirrell, M. V. Structure and rheology of polyelectrolyte complex coacervates. *Soft Matter* **2018**, *14*, 2454−2464.
(31) Spruijt, E.; Sprakel, J.; Cohen Stuart, M. A.; van der Gucht, J. Interfacial tension between a complex coacervate phase and its coexisting aqueous phase. *Soft Matter* **2010**, *6*, 172−178.
(32) Qin, J.; Priftis, D.; Farina, R.; Perry, S. L.; Leon, L.; Whitmer, J.; Hoffmann, K.; Tirrell, M.; De Pablo, J. J. Interfacial tension of polyelectrolyte complex coacervate phases. *ACS Macro Lett.* **2014**, *3*, 565−568.
(33) Knoerdel, A. R.; Blocher McTigue, W. C.; Sing, C. E. Transfer Matrix Model of pH Effects in Polymeric Complex Coacervation. *J. Phys. Chem. B* **2021**, *125*, 8965−8980.
(34) Adhikari, S.; Leaf, M. A.; Muthukumar, M. Polyelectrolyte complex coacervation by electrostatic dipolar interactions. *J. Chem. Phys.* **2018**, *149*, 163308.
(35) Zhang, H.; Elbaum-Garfinkle, S.; Langdon, E. M.; Taylor, N.; Occhipinti, P.; Bridges, A. A.; Brangwynne, C. P.; Gladfelter, A. S. RNA controls PolyQ protein phase transitions. *Molecular cell* **2015**, *60*, 220−230.
(36) Priftis, D.; Xia, X.; Margossian, K. O.; Perry, S. L.; Leon, L.; Qin, J.; de Pablo, J. J.; Tirrell, M. Ternary, tunable polyelectrolyte complex fluids driven by complex coacervation. *Macromolecules* **2014**, *47*, 3076−3085.
(37) Friedowitz, S.; Lou, J.; Barker, K. P.; Will, K.; Xia, Y.; Qin, J. Looping-in complexation and ion partitioning in nonstoichiometric polyelectrolyte mixtures. *Sci. Adv.* **2021**, *7*, No. eabg8654.
(38) Donnan, F.; Guggenheim, E. Exact thermodynamics of membrane equilibrium. *Z. Phys. Chem. A* **1932**, *162*, 346−360.
(39) Li, L.; Srivastava, S.; Meng, S.; Ting, J. M.; Tirrell, M. V. Effects of non-electrostatic intermolecular interactions on the phase behavior of pH-sensitive polyelectrolyte complexes. *Macromolecules* **2020**, *53*, 7835−7844.
(40) Zhang, P.; Alsaifi, N. M.; Wu, J.; Wang, Z.-G. Polyelectrolyte complex coacervation: Effects of concentration asymmetry. *J. Chem. Phys.* **2018**, *149*, 163303.
(41) Rubinstein, M.; Liao, Q.; Panyukov, S. Structure of liquid coacervates formed by oppositely charged polyelectrolytes. *Macromolecules* **2018**, *51*, 9572−9588.
(42) Danielsen, S. P.; Panyukov, S.; Rubinstein, M. Ion pairing and the structure of gel coacervates. *Macromolecules* **2020**, *53*, 9420−9442.
(43) Bobbili, S. V.; Milner, S. T. A simple simulation model for complex coacervates. *Soft Matter* **2021**, *17*, 9181−9188.
(44) Manning, G. S. Limiting laws and counterion condensation in polyelectrolyte solutions I. Colligative properties. *J. Chem. Phys.* **1969**, *51*, 924−933.
(45) Bobbili, S. V.; Milner, S. T. Simulation study of entanglement in semiflexible polymer melts and solutions. *Macromolecules* **2020**, *53*, 3861−3872.
(46) Abraham, M. J.; van der Spoel, D.; Lindahl, E.; Hess, A. The GROMACS development team. *GROMACS* user manual ver. 5.1.5, www.gromacs.org, 2017.
(47) Danielsen, S. P.; McCarty, J.; Shea, J.-E.; Delaney, K. T.; Fredrickson, G. H. Small ion effects on self-coacervation phenomena in block polyampholytes. *J. Chem. Phys.* **2019**, *151*, 034904.
(48) Shusharina, N.; Zhulina, E.; Dobrynin, A.; Rubinstein, M. Scaling theory of diblock polyampholyte solutions. *Macromolecules* **2005**, *38*, 8870−8881.
(49) Wang, Z.; Rubinstein, M. Regimes of conformational transitions of a diblock polyampholyte. *Macromolecules* **2006**, *39*, 5897−5912.

https://doi.org/10.1021/acs.macromol.1c02115
Macromolecules 2022, 55, 511−516